

## Supporting Information

**Two mixed-ligand Cd(II)-organic frameworks with unique topologies:**

**Selective luminescent sensing of TNP and Cu<sup>2+</sup> ions with recyclable performances**

**Jin Fang Zhang<sup>a,\*</sup>, Wen Jia<sup>a</sup>, Junjie Wu<sup>a</sup>, Guodong Tang<sup>b</sup>, Chi Zhang<sup>a,\*</sup>**

*<sup>a</sup>International Joint Research Center for Photoresponsive Molecules and Materials, School of Chemical and Material Engineering, Jiangnan University, Wuxi 214122, P. R. China*

*<sup>b</sup>Jiangsu Key Laboratory for Chemistry of Low-Dimensional Materials, Huaiyin Normal University, Huaian 223300, P. R. China*

## Table of contents

1. **Fig. S1** The asymmetric unit of **1** (a) and **2** (b).
2. **Fig. S2** 3-D packing diagram of **2** viewed approximately along the *a* axis (a) and *b* axis (b).
3. **Fig. S3** The PXRD patterns of **1** (a) and **2** (b).
4. **Fig. S4** PXRD patterns of **1** in different situations.
5. **Fig. S5** Thermogravimetric analysis of **1** and **2**.
6. **Fig. S6-S10** Emission spectra of **1** dispersed in DMF with the addition of different NACs solutions (5 mM) ( $\lambda_{\text{ex}} = 357$  nm).
7. **Fig. S11-S16** Stern-Volmer plots for different NACs of **1** in DMF suspension at the low concentration (0-0.020 mM).
8. **Fig. S17-S22** The detection limits for different NACs of **1** in DMF suspension was calculated with  $3\sigma/k$  (*k*: slope,  $\sigma$ : standard) at the low concentration (0-0.020 mM).
9. **Fig. S23** Spectral overlap between the absorption spectra of 1,3-DNB, 2,4-DNT, 4-NP, 4-NT, NB, TNP and the emission spectra of **1** in DMF and H<sub>2</sub>O media.
10. **Fig. S24** Emission spectra of **1** in aqueous solutions of different cations ( $\lambda_{\text{ex}} = 357$  nm).
11. **Fig. S25** Emission spectra of **1** in aqueous solutions of mixed cations. The concentrations of Cu<sup>2+</sup> and other anions were 2 mM, respectively ( $\lambda_{\text{ex}} = 357$  nm).
12. **Fig. S26** The IR spectra of **1** before and after detection of Cu<sup>2+</sup>.
13. **Table S1** Selected bond lengths (Å) and angles (deg) for **1** and **2**.
14. **Table S2** The ICP results of **1@CuCl<sub>2</sub>**.

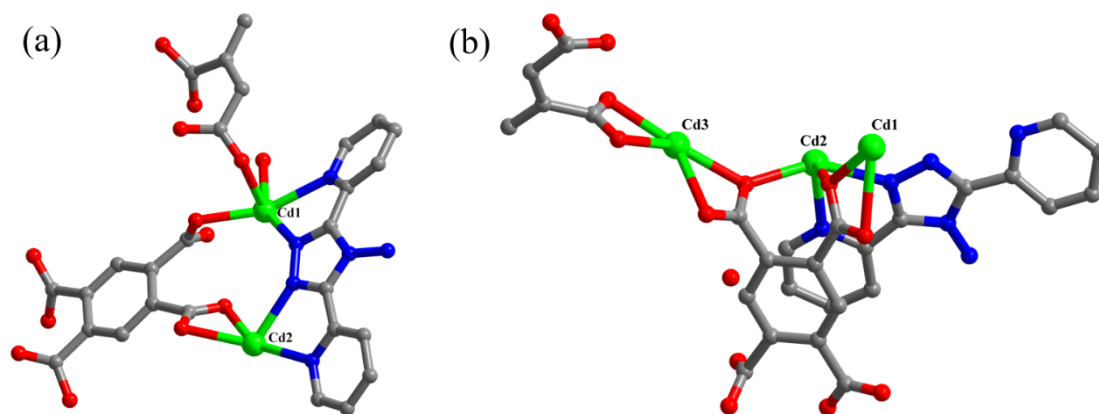


**Fig. S1** The asymmetric unit of **1** (a) and **2** (b). All H atoms are omitted for clarity. Colour code: Cd green, C grey, O red, N blue.

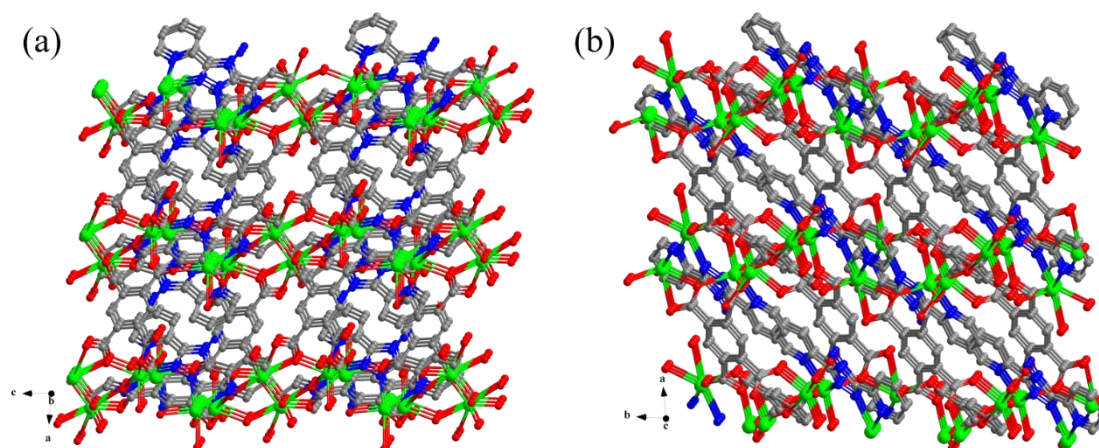


**Fig. S2** 3-D packing diagram of **2** viewed approximately along the *b* axis (a) and *c* axis (b). All H atoms are omitted for clarity. Colour code: Cd green, C grey, O red, N blue.

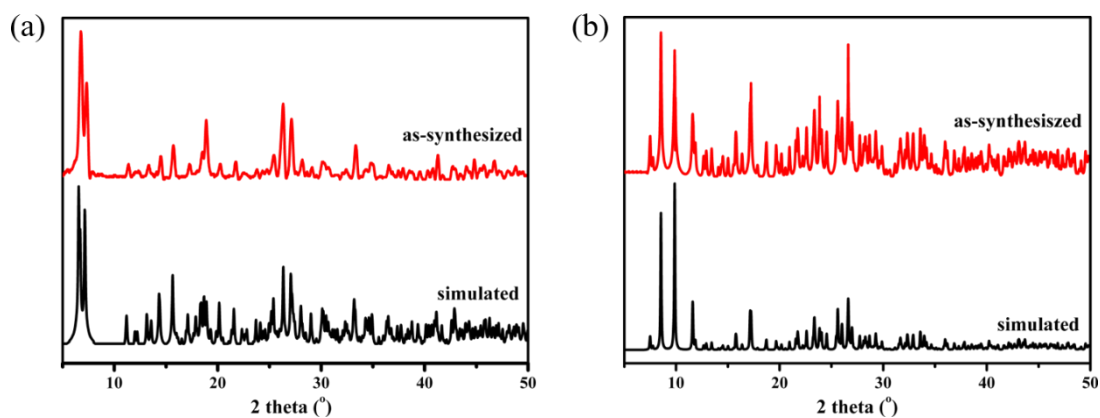


**Fig. S3** The PXRD patterns of **1** (a) and **2** (b).

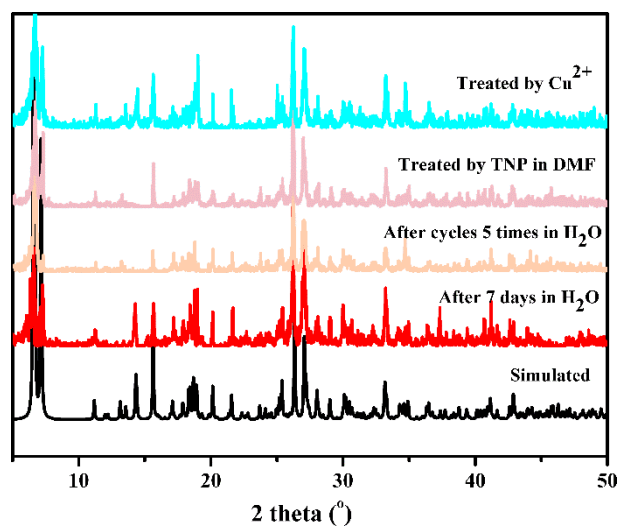


**Fig. S4** PXRD patterns of **1** in different situations.

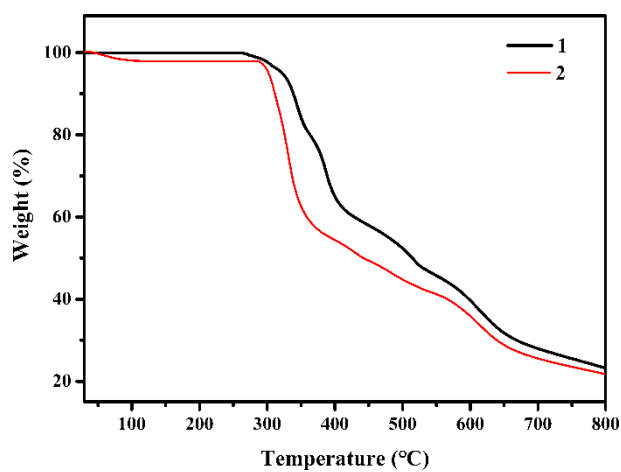


**Fig. S5** Thermogravimetric analysis of **1** and **2**.

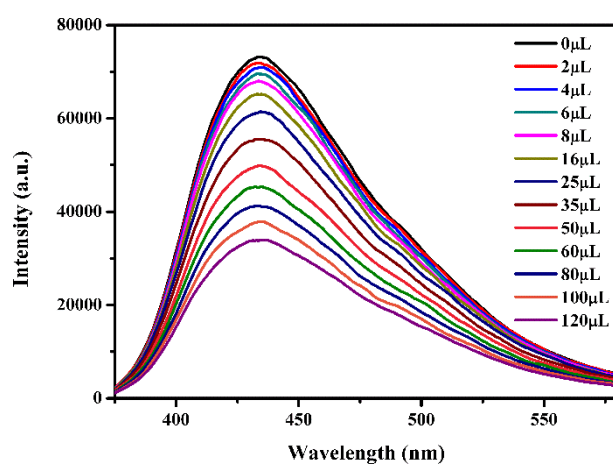


**Fig. S6** Emission spectra of **1** dispersed in DMF with the addition of 4-NP solution (5 mM) ( $\lambda_{\text{ex}} = 357$  nm).

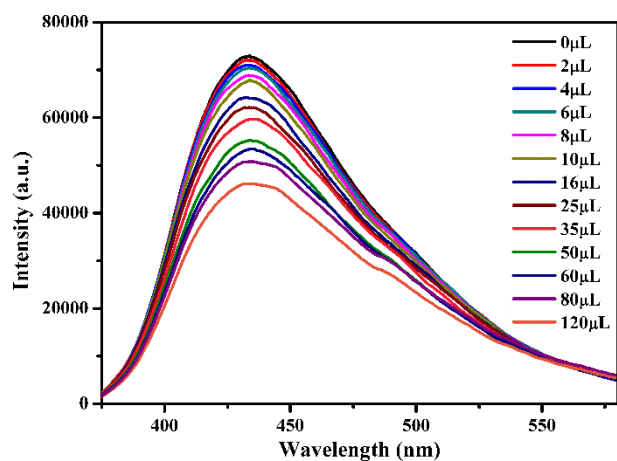


**Fig. S7** Emission spectra of **1** dispersed in DMF with the addition of 2,4-DNT solution (5 mM) ( $\lambda_{\text{ex}} = 357$  nm).

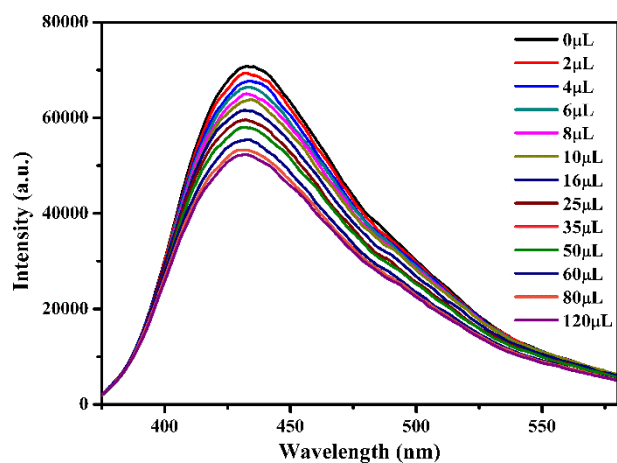


**Fig. S8** Emission spectra of **1** dispersed in DMF with the addition of NB solution (5 mM) ( $\lambda_{\text{ex}} = 357$  nm).

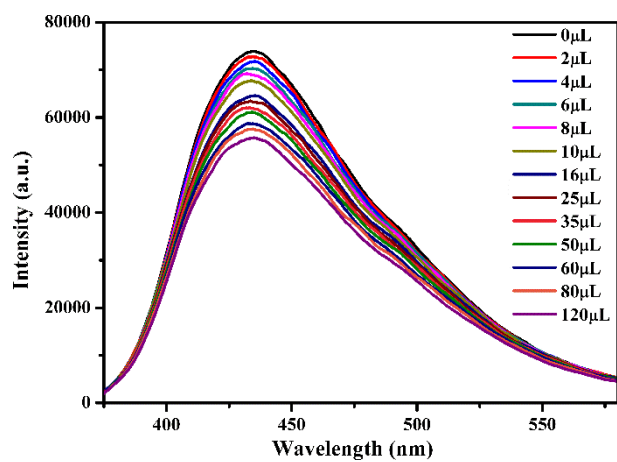


**Fig. S9** Emission spectra of **1** dispersed in DMF with the addition of 4-NT solution (5 mM) ( $\lambda_{\text{ex}} = 357$  nm).

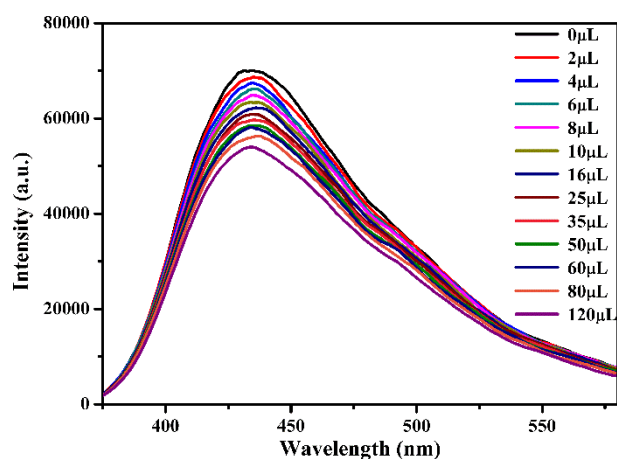


**Fig. S10** Emission spectra of **1** dispersed in DMF with the addition of 1,3-DNB solution (5 mM) ( $\lambda_{\text{ex}} = 357$  nm).

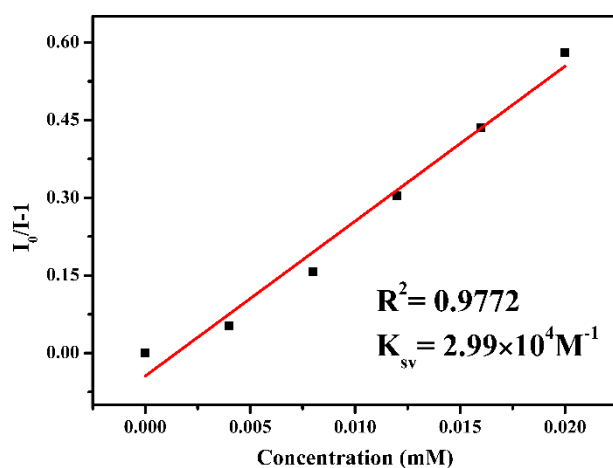


**Fig. S11** Stern-Volmer plot for TNP of **1** in DMF suspension at the low concentration (0-0.020 mM).

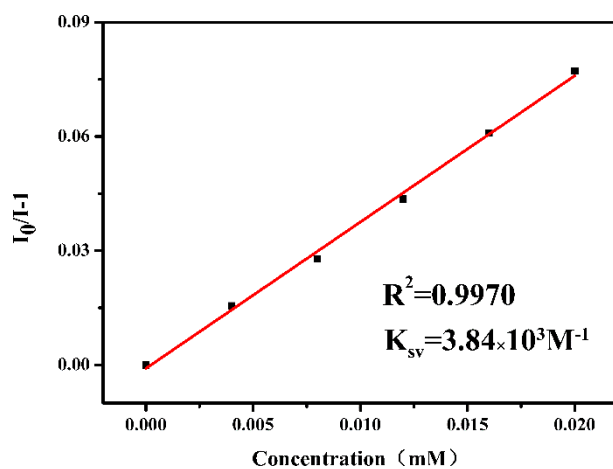


**Fig. S12** Stern-Volmer plot for 4-NP of **1** in DMF suspension at the low concentration (0-0.020 mM).

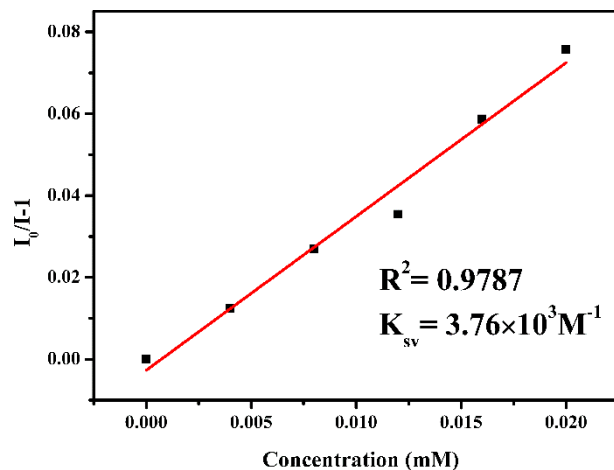


**Fig. S13** Stern-Volmer plot for 2,4-DNT of **1** in DMF suspension at the low concentration (0-0.020 mM).

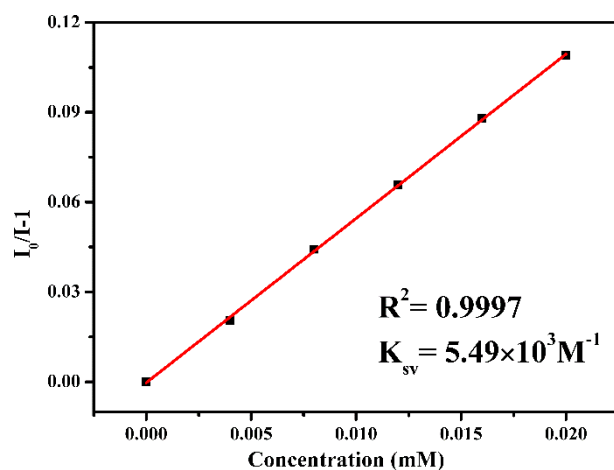


**Fig. S14** Stern-Volmer plot for NB of **1** in DMF suspension at the low concentration (0-0.020 mM).

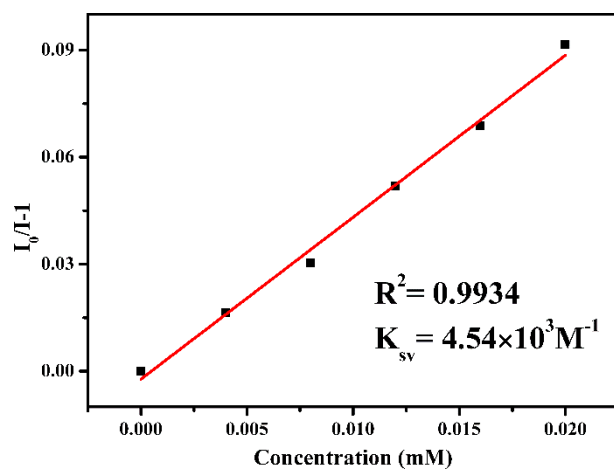


**Fig. S15** Stern-Volmer plot for 4-NT of **1** in DMF suspension at the low concentration

(0-0.020 mM).

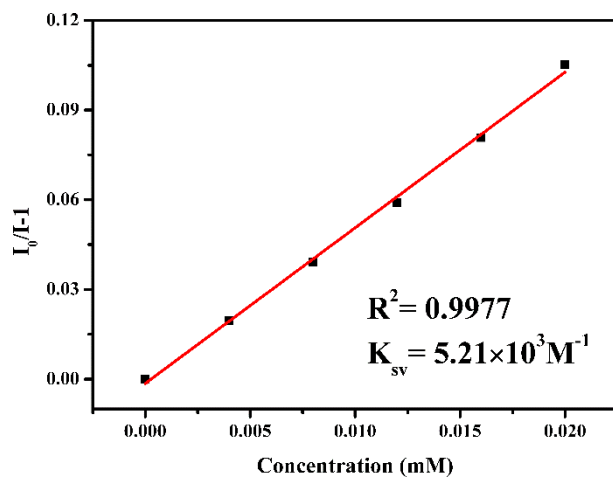


**Fig. S16** Stern-Volmer plot for 1,3-DNB of **1** in DMF suspension at the low concentration (0-0.020 mM).

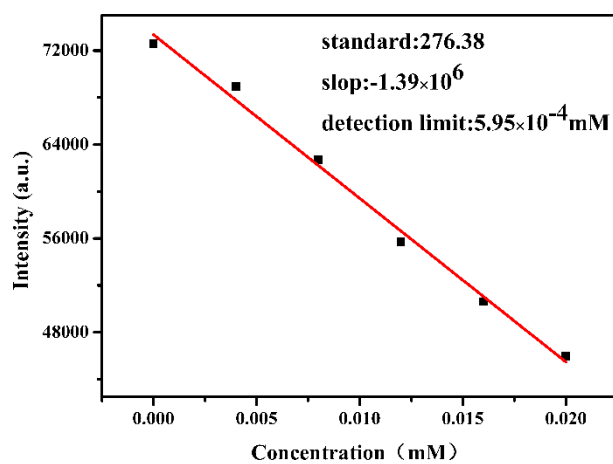


**Fig. S17** The LOD for TNP of **1** in DMF suspension was calculated with  $3\sigma/k$  ( $k$ : slope,  $\sigma$ : standard) at the low concentration (0-0.020 mM).

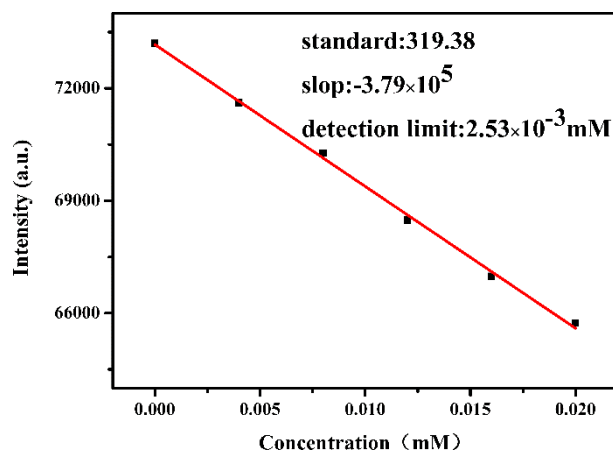




**Fig. S18** The LOD for 4-NP of **1** in DMF suspension was calculated with  $3\sigma/k$  ( $k$ : slope,  $\sigma$ : standard) at the low concentration (0-0.020 mM).

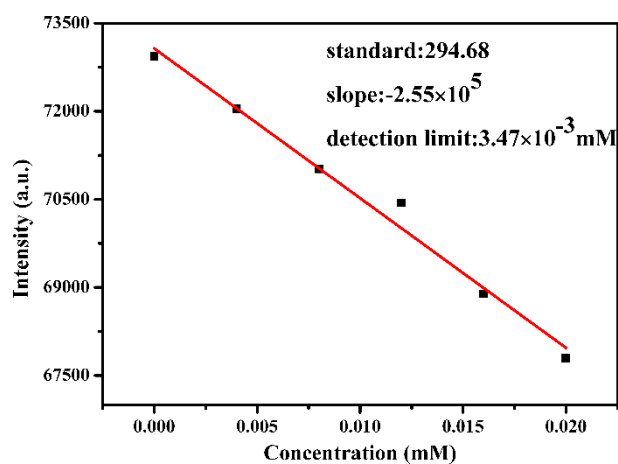


**Fig. S19** The LOD for 2,4-DNT of **1** in DMF suspension was calculated with  $3\sigma/k$  ( $k$ : slope,  $\sigma$ : standard) at the low concentration (0-0.020 mM).

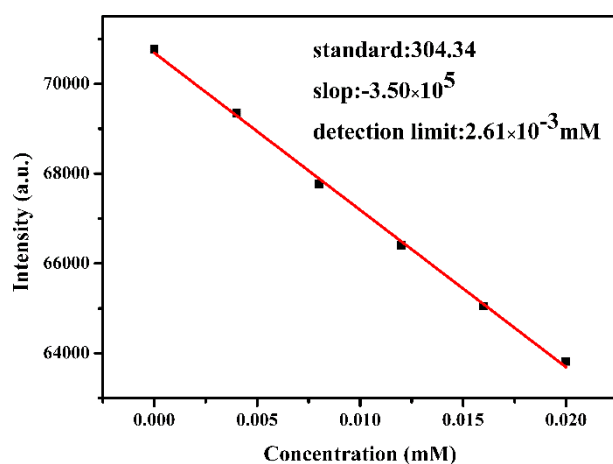


**Fig. S20** The LOD for NB of **1** in DMF suspension was calculated with  $3\sigma/k$  ( $k$ : slope,  $\sigma$ : standard) at the low concentration (0-0.020 mM).

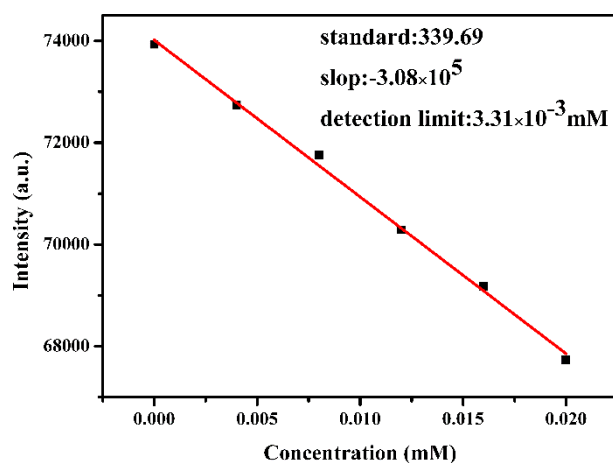


**Fig. S21** The LOD for 4-NT of **1** in DMF suspension was calculated with  $3\sigma/k$  ( $k$ : slope,  $\sigma$ : standard) at the low concentration (0-0.020 mM).

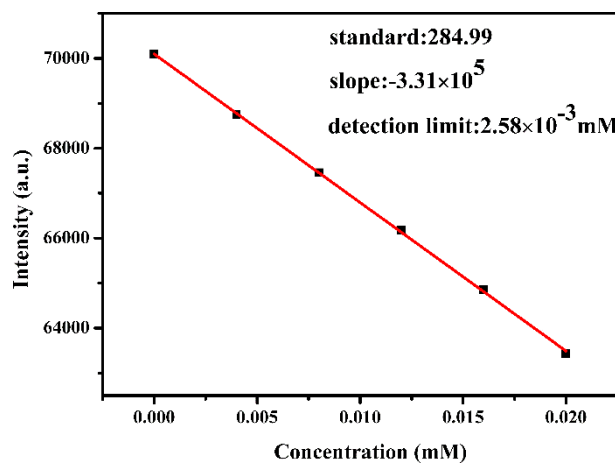


**Fig. S22** The LOD for 1,3-DNB of **1** in DMF suspension was calculated with  $3\sigma/k$  ( $k$ : slope,  $\sigma$ : standard) at the low concentration (0-0.020 mM).

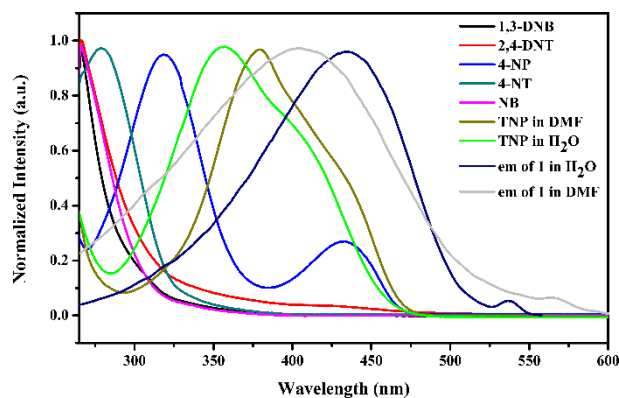


**Fig. S23** Spectral overlap between the absorption spectra of 1,3-DNB, 2,4-DNT, 4-NP, 4-NT, NB, TNP and the emission spectra of **1** in DMF and H<sub>2</sub>O media.

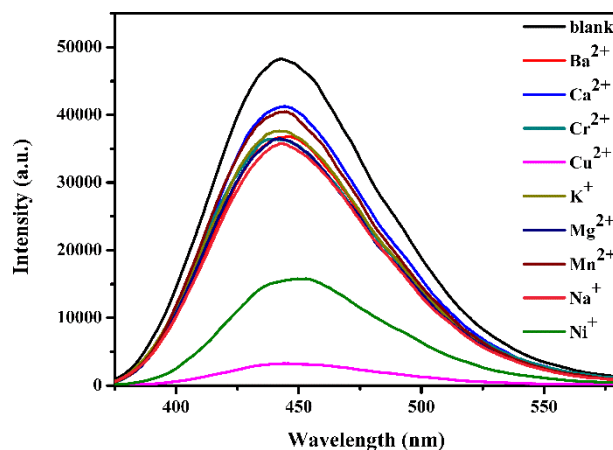


**Fig. S24** Emission spectra of **1** in aqueous solutions of different cations ( $\lambda_{\text{ex}} = 357$  nm).

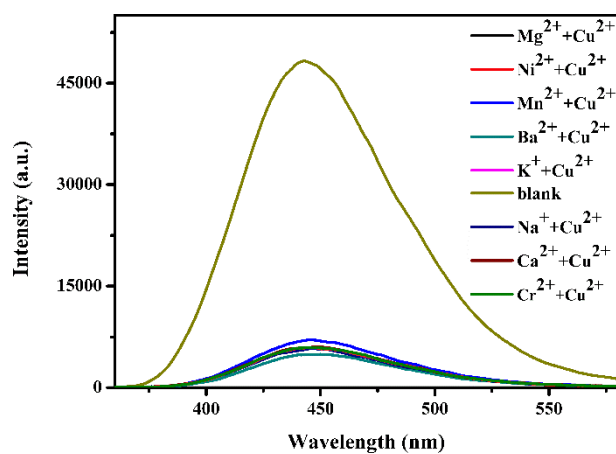


**Fig. S25** Emission spectra of **1** in aqueous solutions of mixed cations. The concentrations of Cu<sup>2+</sup> and other anions were 2 mM, respectively ( $\lambda_{\text{ex}} = 357$  nm).

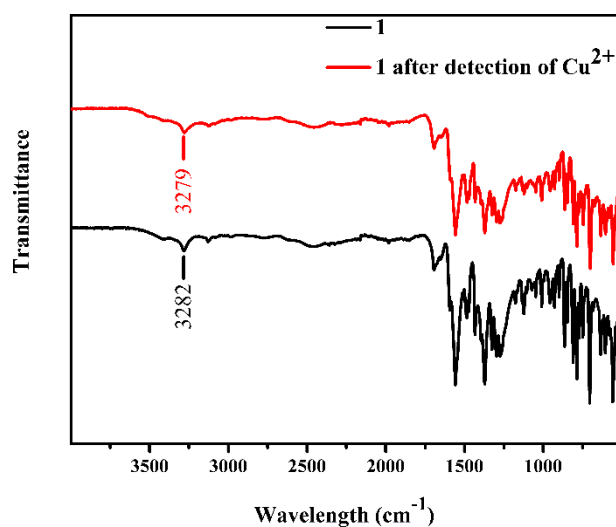


**Fig. S26** The IR spectra of **1** before and after detection of Cu<sup>2+</sup>.

**Table S1** Selected bond lengths (Å) and angles (deg) for **1** and **2**.

Bond	Lengths (Å)	Bond	Angles (°)
<b>1</b>			
Cd(1)-N(2)	2.314(2)	N(2)-Cd(1)-O(6)	153.10(8)
Cd(1)-O(6)	2.354(2)	N(2)-Cd(1)-O(4)	87.95(7)
Cd(2)-O(3)	2.293(2)	O(13)#1-Cd(1)-N(2)	87.30(8)
Cd(2)-O(1)	2.410(2)	O(1)-Cd(1)-O(13)#1	105.50(7)
Cd(1)-N(1)	2.410(2)	O(1)-Cd(1)-O(4)	79.67(7)
Cd(1)-O(4)	2.3176(19)	O(1)-Cd(1)-O(6)	91.52(7)
Cd(1)-O(1)	2.2496(19)	O(4)-Cd(1)-O(6)	89.80(7)
Cd(1)-O(13)#1	2.2868(19)	N(2)-Cd(1)-N(1)	70.32(8)
O(1)-Cd(1)-N(1)	159.92(8)	O(1)-Cd(1)-N(2)	114.38(8)
<b>2</b>			
O(4)-Cd(3)#4	2.467(4)	N(5B)#1-Cd(1)-O(1)	139.2(7)
Cd(1)-O(5)#2	2.262(4)	N(4A)-Cd(2)-N(1A)	71.0(2)
O(1)-Cd(2)	2.440(4)	O(3)-Cd(2)-O(9)#5	82.86(14)
Cd(2)-N(4A)	2.208(6)	O(1)-Cd(1)-O(2)	52.15(13)
Cd(2)-O(9)#5	2.335(4)	O(5)#2-Cd(1)-O(2)	79.95(17)
O(8)-Cd(3)	2.155(4)	O(12)#3-Cd(1)-O(1)	127.02(16)
Cd(1)-O(2)	2.623(5)	O(5)#2-Cd(1)-O(1)	97.00(15)
O(9)-Cd(3)	2.374(4)	N(6B)#1-Cd(1)-O(1)	76.9(5)
Cd(2)-O(3)	2.229(4)	O(12)#3-Cd(1)-O(2)	82.19(15)
Cd(1)-O(12)#3	2.304(5)	O(3)-Cd(2)-N(1B)	104.0(5)
Cd(1)-O(1)	2.336(4)	O(3)-Cd(2)-N(1A)	92.4(2)

Symmetry transformations used to generate equivalent atoms: **1**: #1 -x-1/2, y-1/2, -z-1/2. **2**: #1 -x, -y, -z+1; #2 -x+1, -y, -z+1; #3 -x+1, -y, -z; #4 x-1, y, z; #5 -x+1, -y+1, -z.

**Table S2** The ICP results of **1@CuCl<sub>2</sub>** (50 mg compound soaked in 2 mL of 2 mM CuCl<sub>2</sub> for 24 hours).

Sample	Concentration/(mg/kg)	Determined ion
<b>1@CuCl<sub>2</sub></b>	175424	Cd <sup>2+</sup>
<b>1@CuCl<sub>2</sub></b>	176271	Cd <sup>2+</sup>
<b>1@CuCl<sub>2</sub></b>	1864	Cu <sup>2+</sup>
<b>1@CuCl<sub>2</sub></b>	1856	Cu <sup>2+</sup>

Results analysis:

the ratio of Cd<sup>2+</sup> : Cu<sup>2+</sup> in **1@CuCl<sub>2</sub>** : [(175424+176271)/2] : [(1864+1856)/2] = 94.54 : 1